

Ultra-high energy cosmic rays, cascade γ -rays, and high-energy neutrinos from gamma-ray bursts

C D Dermer¹ & A Atoyan²

¹Space Science Division Code 7653 4555 Overlook Ave. SW Washington DC 20375
USA

E-mail: dermer@gamma.nrl.navy.mil

²Centre de Recherches Mathématiques Université de Montréal Montréal Canada H3C
3J7

E-mail: atoyan@crm.umontreal.ca

Abstract. Gamma-ray bursts (GRBs) are sources of energetic, highly variable fluxes of γ rays, which demonstrates that they are powerful particle accelerators. Besides relativistic electrons, GRBs should also accelerate high-energy hadrons, some of which could escape cooling to produce ultra-high energy cosmic rays (UHECRs). Acceleration of high-energy hadrons in GRB blast waves will be established if high-energy neutrinos produced through photopion interactions in the blast wave are detected from GRBs. Limitations on the energy in nonthermal hadrons and the number of expected neutrinos are imposed by the fluxes from pair-photon cascades initiated in the same processes that produce neutrinos. Only the most powerful bursts at fluence levels $\gtrsim 3 \times 10^{-4}$ erg cm⁻² offer a realistic prospect for detection of \gg TeV neutrinos. Detection of high-energy neutrinos is likely if GRB blast waves have large baryon loads and Doppler factors $\lesssim 200$. Cascade γ rays will accompany neutrino production and might already have been detected as anomalous emission components in the spectra of some GRBs. Prospects for detection of GRBs in the Milky Way are also considered.

1. Introduction

There is general consensus that acceleration of cosmic rays by supernova remnants (SNRs) is the main source of galactic cosmic rays at energies below ~ 100 TeV (e.g., [1]). It is also generally thought that all cosmic rays with energies up to at least the second knee in the cosmic-ray spectrum at $E_2 \sim 3 \times 10^{17}$ eV (e.g. [2]) or even up to the ankle at $E_{\text{ank}} \simeq 3 \times 10^{18}$ eV are produced in our Galaxy (see, e.g., [3]). Meanwhile, cosmic-ray acceleration to energies significantly exceeding $\approx 10^{14}$ eV with the conventional mechanism of nonrelativistic first-order shock acceleration by SNRs from typical (Type Ia and II) supernovae (SNe) is problematic [4]. The origin of the knee in the cosmic-ray spectrum in the form of a spectral-index break in the power-law all-particle spectrum by ≈ 0.3 units at $E_1 \simeq 3 \times 10^{15}$ eV, accompanied by a change in the cosmic-ray composition, seems to suggest a new contribution to cosmic rays at these energies.

GRBs have been proposed as effective accelerators of cosmic rays in the universe [5] and as probable sources of cosmic rays up to ultra-high energies in our Galaxy [6]. Cosmic rays with energies below ~ 100 TeV are produced in the conventional scenario of continuous injection due to nonrelativistic shock acceleration by SNRs formed in all types of SNe, with subsequent modification of the source spectrum through energy-dependent propagation (see [1, 7]). GRBs in our own Galaxy are very rare and probably take place at a rate $\lesssim 10^{-4}$ yr $^{-1}$. Our best opportunity to establish cosmic-ray acceleration in GRB blast waves is by looking for hadronic emission signatures in the spectra of GRBs, or characteristic signatures from remnants of past GRBs. Conclusive evidence for cosmic-ray acceleration in GRBs will come from the detection of high-energy neutrinos.

In the relativistic blast-wave model for GRBs, photohadronic production is the most important mechanism for producing high-energy neutrinos. In Section 2, the photohadron process is described and an approximation used for computing the spectra of secondaries formed in photohadronic processes, which is also useful for analytical studies, is given. Calculations of secondary neutrino and cascade gamma-ray production are presented in Section 3, and the requirements for detection of high-energy neutrinos from GRBs are derived. Models for UHECRs from GRBs are described in Section 4. A discussion of signatures of GRBs in the Galaxy is found in Section 5, where we briefly consider recent reports that GRBs favor sites of low metallicity. Summary and conclusions are given in Section 6.

2. Photohadronic Processes

If high-energy hadrons are accelerated by GRB blast waves, then photohadronic processes, which require the presence of target photons, are the most important hadronic energy-loss mechanisms. The target photon field is simply the highly variable radiation formed in the GRB blast wave that is detected as the GRB. Secondary nuclear

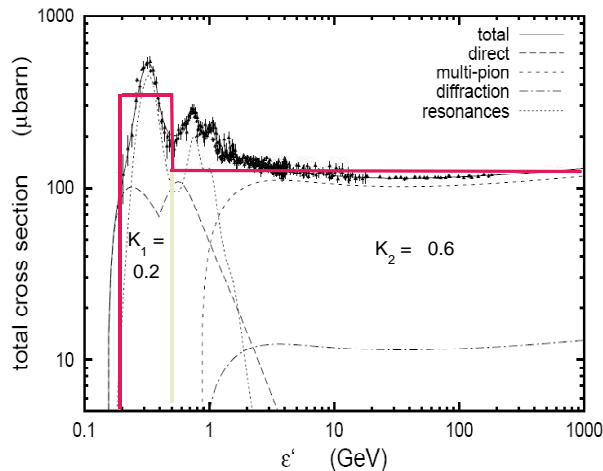


Figure 1. The total $p\gamma$ photomeson cross section as a function of the photon's energy in the proton rest frame [10] ($1\mu\text{barn} = 10^{-30} \text{ cm}^2$; data from Ref. [11] and references therein). The contributions of baryon resonances, the direct single-pion channel, diffractive scattering, and multipion production are shown separately. Also shown is the two step-function approximation used in calculations.

production, by contrast, requires a large target particle density that would make the GRB energetics untenable [8].

The most important photohadronic process for hadronic energy losses in GRB blast waves is the photopion reaction, which can be written as $p + \gamma \rightarrow N + \pi$, where N stands for a proton or neutron. Another important photohadronic process is photopair production, which can be written as $p + \gamma \rightarrow p + e^+ + e^-$. A large fraction of the initial proton energy is lost in a photopion reaction, so only a few scatterings are required for the proton to lose most of its initial energy. By contrast, only a small fraction of the initial proton energy is lost in photopair production, so hundreds of scatterings are needed for a proton to lose most of its initial energy through this process. Although the photopair reaction is not so important for hadronic energy losses in GRB blast waves, it can play an important role in the evolution of the UHECR spectrum throughout intergalactic space [9].

The photopion process $p + \gamma \rightarrow N + \pi$ has a threshold photon energy $\epsilon_{th} = m_\pi + m_\pi^2/2m_p \cong 150 \text{ MeV}$, and its cross section is shown in Fig. 1. Four separate contributions to the total photopion cross section [10] are shown, namely resonance production involving, for example, the $\Delta^+(1232)$ resonance; direct production, which refers to residual, nonresonant contributions to direct two-body channels; multi-pion production; and diffractive scattering.

A useful approximation [8] to the photopion process is to treat it as the sum of two channels, namely the *single-pion resonance channel*, where the proton loses 20% of its

energy on average through the reaction

$$p + \gamma \rightarrow \Delta^+ \rightarrow \begin{cases} p + \pi^0 \rightarrow p + 2\gamma \\ n + \pi^+ \rightarrow n + e^+ + 3\nu \end{cases},$$

and a *multi-pion channel*, where the proton loses on average 60% of its initial energy. The latter channel is assumed to be equally divided into secondary $\pi^0, \pi^+,$ and π^- particles. In the $p + \gamma \rightarrow \Delta^+ \rightarrow p + \pi^0$ channel, the neutral pion decays into two γ rays with $\approx 10\%$ of the energy of the initial proton. Following production, the γ rays will usually convert into e^+e^- pairs through the $\gamma\gamma \rightarrow e^+e^-$ absorption processes, initiating an electromagnetic synchrotron/Compton/pair-production cascade.

In the $p + \gamma \rightarrow \Delta^+ \rightarrow n + \pi^+$ channel, the decay of the charged pion produces three neutrinos and a positron in the reaction chain

$$\pi^+ \rightarrow \mu^+ + \nu_\mu, \text{ followed by the decay } \mu^+ \rightarrow e^+ + \nu_e + \bar{\nu}_\mu.$$

Unless the neutron first interacts with a photon through the photohadronic process and is converted into a proton, it decays with a mean lifetime $t_n \cong 886$ s [12] in the rest frame through the β -decay reaction

$$n \rightarrow p + e^- + \bar{\nu}_e.$$

The β -decay electron and neutrino have energies ≈ 1 MeV in the neutron's rest frame. In a single $p\gamma$ interaction leading to the production of a single π^+ , four ν and two leptons are therefore formed, with one of the neutrinos and one of the leptons having $\approx 50\times$ less energy than the others.

The two-step function approximation [8, 13] for the photopion cross section is given by

$$\sigma_{p\gamma}(\epsilon_r) = \begin{cases} 340 \mu\text{b}, & \epsilon_{th} = 390 \leq \epsilon_r \leq 980 \\ 120 \mu\text{b}, & \epsilon_r > 980 \end{cases} \quad (1)$$

and inelasticity

$$K_{p\gamma}(\epsilon_r) = \begin{cases} 0.2, & 390 \leq \epsilon_r \leq 980 \\ 0.6, & \epsilon_r > 980 \end{cases}, \quad (2)$$

as shown in Fig. 1. Hence

$$\sigma_{p\gamma}(\epsilon_r)K_{p\gamma}(\epsilon_r) \equiv \sigma_1 K_1 \cong 70H(\epsilon_r - 390) \mu\text{b}. \quad (3)$$

In this approximation, the lower-energy step function approximates the $\Delta(1232)$ resonance production process, and the higher-energy step function approximates the multi-photon production process. For the Δ resonance, isospin statistics imply [14] a charge-changing ratio of 1/3 for single resonance production. Thus the probability of the processes $p\gamma \rightarrow n\pi^+$ and $p\gamma \rightarrow p\pi^0$ is in the ratio 1 : 2. In the multi-pion limit, the production of π^+, π^- and π^0 approaches 1 : 1 : 1.

3. Neutrinos and Cascade Gamma Rays

Much effort has been devoted to understanding radiative signatures of leptons accelerated in GRB blast waves (e.g., [15]), and this approach can also be applied to hadronic acceleration [16]. Consider a GRB blast wave with Lorentz factor Γ . Relativistic protons or hadrons are assumed to be injected in the comoving frame of the blast wave with a number spectrum $\propto E_p^{-s}$ at comoving proton energies $E_p > \Gamma$ GeV up to a maximum proton energy determined by the condition that the particle Larmor radius is smaller than both the size scale of the emitting region and the photomeson energy-loss length. The injection index $s \approx 2.2$, as suggested by relativistic shock acceleration and particle injection determined by analyses of GRB afterglows [17].

The total photon fluence $\Phi = \int_{-\infty}^{\infty} dt \int_0^{\infty} dE E \phi(E, t)$ of a GRB, where $\phi(E, t)$ is the differential photon number flux, must be at the level of $\Phi \gtrsim 10^{-4}$ ergs cm^{-2} to be detected with a km-scale neutrino telescope such as IceCube, as we now show. For the detection of N_{ν_μ} muon neutrinos, the best sensitivity of a neutrino telescope for detecting a spectrum of neutrinos that is falling $\propto \epsilon_\nu^{-p}$ with $p > 1$ is near 100 TeV ≈ 160 ergs. This is because of the linear increase of the detection probability $P_{\nu_\mu}(\epsilon_\nu) \approx 10^{-4}(\epsilon_\nu/100 \text{ TeV})$ at $\epsilon_\nu \gtrsim 1$ TeV [18], and the increasingly large cosmic-ray induced neutrino background at $\epsilon_\nu \ll 100$ TeV. The detection of N_{ν_μ} neutrinos therefore requires that the neutrino fluence $\Phi_{\nu_\mu} \simeq (160 \text{ ergs})N_{\nu_\mu}/[P_{\nu_\mu}(100 \text{ TeV}) \cdot 10^{10} \text{ cm}^2] \approx 10^{-4}N_{\nu_\mu}$ ergs cm^{-2} . Because the differential neutrino fluence $E^2 \phi_\nu(E) = E^2 \int_{-\infty}^{\infty} dt \phi_\nu(E, t)$, where $\phi_\nu(E)$ is the differential neutrino number flux, will be spread over several orders of magnitude, it is necessary that $\Phi \gtrsim 10^{-4}$ ergs cm^{-2} in order to produce a sufficient neutrino fluence for detection, given that the ν_μ fluence will generally be smaller than the photon fluence even in the optimistic case that the photon radiation originates substantially from hadronic processes.

In calculations presented here to illustrate the astrophysical importance of photomeson production and subsequent electromagnetic cascades, the observed synchrotron spectral flux in the prompt phase of the burst is parameterized, as shown in Fig. 2, by the expression $F(\nu) \propto \nu^{-1}(\nu/\nu_{br})^\alpha$, where $h\nu_{br} = 300$ keV, $\alpha = -0.5$ above ν_{br} and an exponential cutoff at 10 MeV, and $\alpha = 0.5$ when $10 \text{ keV} \leq h\nu \leq h\nu_{br}$. At lower energies, $\alpha = 4/3$. The observed total hard X-ray (keV – MeV) photon fluence $\Phi_{tot} \cong t_{dur} \int_0^{\infty} d\nu F(\nu)$, where t_{dur} is the characteristic duration of the GRB. We consider a source at redshift $z = 1$ and assume the hard X-ray fluence $\Phi_{tot} \gtrsim 3 \times 10^{-4}$ erg cm^{-2} . One or two GRBs should occur each year above this fluence level. Here we take $s = 2$.

A total amount of energy $E' = 4\pi d_L^2 f_{CR} \Phi_{tot} \delta^{-3} (1+z)^{-1}$ is injected in the form of accelerated proton energy into the comoving frame of the GRB blast wave. Here z is the redshift, d_L is the luminosity distance, and

$$\delta = \frac{1}{\Gamma(1 - \beta\mu)} \quad (4)$$

is the Doppler factor. The factor f_{CR} is the baryon-loading factor, which gives the ratio of energy deposited in nonthermal hadrons compared to the energy detected as

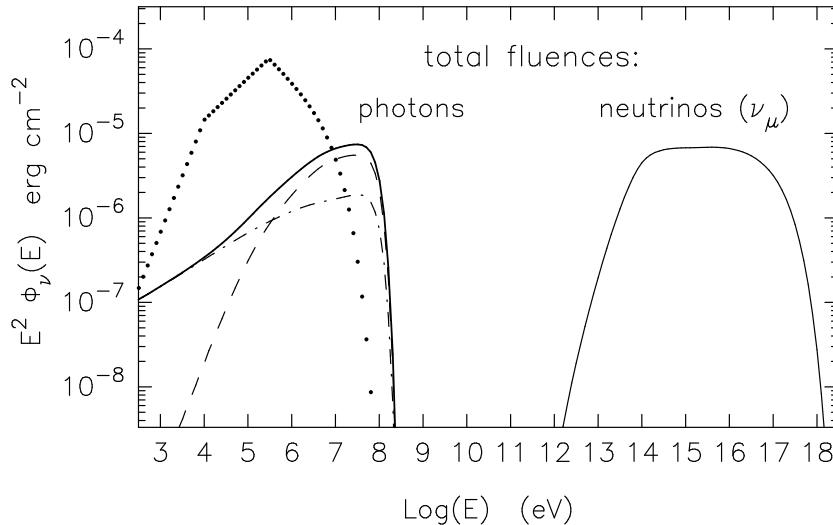


Figure 2. Differential energy fluence of photons and photomeson muon neutrinos for a collapsar-model GRB with hard X-ray fluence $\Phi_{tot} = 3 \times 10^{-4}$ erg cm $^{-2}$ and $\delta = 100$. The dotted curve shows the fluence of a GRB used for calculations, and the dashed and dot-dashed curves show the Compton and synchrotron contributions to the photon fluence from the electromagnetic cascade initiated by secondaries from photomeson processes, respectively.

electromagnetic radiation, which is assumed to be provided by nonthermal electrons. The energy deposited into each of N_{sp} light-curve pulses (or spikes) is therefore $E'_{sp} = E'/N_{sp}$ ergs. We assume that all the energy E'_{sp} is injected in the first half of the time interval of the pulse (to ensure variability in the GRB light curve), which effectively corresponds to a characteristic variability time scale $t_{var} = t_{dur}/2N_{sp}$. The proper width of the radiating region forming the pulse is $\Delta R' \cong t_{var}c\delta/(1+z)$, from which the energy density of the synchrotron radiation can be determined [19]. We set the GRB prompt duration $t_{dur} = 100$ s, and let $N_{sp} = 50$, corresponding to $t_{var} = 1$ s.

The magnetic field is determined by assuming equipartition between the energy densities of the magnetic field and the nonthermal electron energies inferred from the synchrotron radiation spectrum. For the parameters considered here, the equipartition magnetic field range from several 100 G to a few kG (depending on δ). For fields $B \gg$ kG, energy losses of the pions and muons can introduce a break in the ν_{μ} spectrum at multi-PeV energies [20], but we neglect that effect in our calculations. The constraint on maximum possible proton energy imposed by the condition that the gyroradius is less than the source size is also imposed. In addition, relativistic expansion of the blast wave causes adiabatic cooling of the particles, which limits neutrino production for a duration set by the blast-wave shell light-crossing time.

In Fig. 3 we show the neutrino fluence expected in the collapsar GRB scenario from a model burst with photon fluence $\Phi_{rad} = 3 \times 10^{-4}$ erg cm $^{-2}$ at redshift $z = 1$. In order to demonstrate the dependence of the neutrino fluxes on δ , we consider 3 values of δ . The

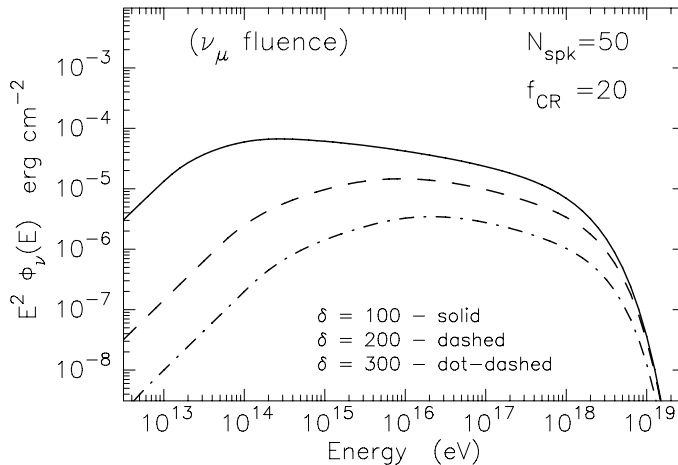


Figure 3. The differential energy fluence of muon neutrinos calculated for a GRB at $z = 1$ with hard X-ray fluence of 3×10^{-4} ergs cm^{-2} and Doppler factors $\delta = 100, 200$ and 300 , and a nonthermal baryon-loading factor $f_{CR} = 20$.

value of f_{CR} is set equal to 20 in this calculation. Here we take $s = 2.2$. The numbers of muon neutrinos that would be detected from a single GRB with IceCube for these parameters and with $\delta = 100, 200$ and 300 are $N_\nu = 1.32, 0.105$ and 0.016 , respectively. We should note, however, that for the assumed value of f_{CR} , the calculated total fluence of neutrinos (both ν_μ and ν_e) produced when $\delta = 100$ is $\Phi_{\nu,tot} = 7.2 \times 10^{-4}$ erg cm^{-2} , i.e., by a factor $7.2/3 = 2.4$ larger than the assumed radiation fluence. This means that the maximum value of the baryon loading that could be allowed if the high-energy radiation fluence is less than the X/ γ fluence for this particular case should be about 8 – 10, instead of 20, in order that the hadronic cascade γ -ray flux is guaranteed not to exceed the measured photon flux. Consequently, the expected number of neutrinos for $\delta = 100$ should be reduced to $\simeq 0.6$. On the other hand, the neutrino fluence for the case $\delta = 200(300)$ is equal to $\Phi_{\nu,tot} = 1.4 \times 10^{-4}(3 \times 10^{-5})$ erg cm^{-2} , so this accommodates an increased baryon-loading from $\lesssim 20$ up to $f_{CR} \simeq 45(200)$, with the expected number of neutrinos observed by IceCube being $N_{\nu,corr} \simeq 0.23(0.16)$. If the radiation fluence at MeV – GeV energies is allowed to exceed the X/ γ fluence by an order of magnitude, a possibility that GLAST will resolve, then the expected number of detected neutrinos could be increased correspondingly.

For the large baryon load $f_{CR} \gtrsim 20$, which is required in the hypothesis that GRBs are the sources of UHECRs, as discussed in the next Section, calculations show that 100 TeV – 100 PeV neutrinos could be detected several times per year from all GRBs with kilometer-scale neutrino detectors such as IceCube [13, 21]. It is important that at these energies the number of atmospheric background neutrinos expected for a km-scale neutrino detector in the time window of a typical long GRB is negligible. Detection of even 1 or 2 neutrinos from GRBs with IceCube or a northern hemisphere neutrino detector will provide compelling support for this scenario for the origin of high-energy and UHE cosmic rays.

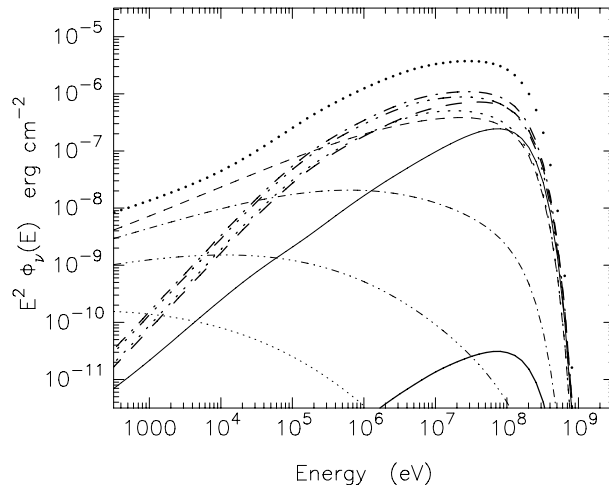


Figure 4. Differential photon energy fluence from an electromagnetic cascade initiated by photopion secondaries in a model GRB, with parameters as given in Fig. 2 and with $\delta = 100$. Five generations of Compton (heavy curves) and synchrotron (light curves) are shown. The first through fifth generations are given by solid, dashed, dot-dashed, dot-triple-dashed, and dotted curves, respectively. The total cascade radiation spectrum is given by the upper bold dotted curve.

A pair-photon cascade initiated by photohadronic processes between high-energy hadrons accelerated in the GRB blast wave and the internal synchrotron radiation field produces a γ -ray emission component that appears during the prompt phase of a GRB, as shown in Fig. 4. The various generations of synchrotron and Compton radiation initiated by the cascade are shown, along with the total radiation spectrum. As can be seen, the cascade radiation approaches the spectrum of an electron distribution cooling by synchrotron losses, that is, a spectrum with photon number index between -1.5 and -2 .

Photomeson interactions in the relativistic blast wave also produce a beam of UHE neutrons, as proposed for blazar jets [8], which may escape from the site of the GRB to deposit UHECRs at distances ranging from the close exterior neighborhood of the blast wave to multi-parsec scales. Subsequent photopion production of these neutrons with photons outside the blast wave can also produce a directed hyper-relativistic electron-positron beam in the process of charged pion decay and the conversion of high-energy photons formed in π^0 decay [22]. These energetic leptons produce a synchrotron spectrum in the radiation reaction-limited regime extending to \gtrsim GeV energies, with properties in the 1 – 200 MeV range similar to that measured from GRB 941017 [23]. Large fluence GRBs displaying these anomalous γ -ray components are most likely to be detected as sources of high-energy neutrinos [24].

Fig. 2 also shows calculations of photomeson neutrino production for a GRB with $\Phi_{tot} = 3 \times 10^{-4}$ erg cm $^{-2}$ and $\delta = 100$, as well as the accompanying electromagnetic radiation induced by pair-photon cascades from the secondary electrons and γ rays

from the same photomeson interactions. The total number of ν_μ expected with IceCube is $\cong 0.1$. The total fluence of cascade photons shown here is contributed by lepton synchrotron (dot-dashed) and Compton (dashed) emissions. For comparison, the dotted curve shows the primary lepton synchrotron radiation spectrum assumed for the calculations. The level of the fluence of the cascade photons is $\approx 10\%$ of the primary synchrotron radiation. This means that the maximum allowed baryon loading for these parameters cannot exceed a factor of ≈ 30 in order not to overproduce the primary synchrotron radiation fluence, as in the case of GRB 941017 [23]. This limits the maximum number of ν_μ to ≈ 3 even in the case of large baryon loading for rare, powerful GRBs, unless a very strong hadronic emission component accompanies the GRB. This component, whose existence is indicated by joint analysis of BATSE and EGRET/TASC data in GRB 941017 and at least two other GRBs [23], will be strongly detected by the GRB Monitor and Large Area Telescope on GLAST.

4. Cosmic Rays from GRBs

The original argument [5] that GRBs are the sources of UHECRs was based on the coincidence between the energy density of UHECRs and the amount of power necessary to supply cosmic rays with energies $\gtrsim 10^{20}$ eV. These GZK cosmic rays, named after the discoverers of the effect [25], are subject to strong photomeson energy losses on cosmic microwave background photons. The effective distance for 10^{20} eV protons to lose 50% of their energy is ≈ 140 Mpc [26], so that the photopion energy-loss timescale of 10^{20} eV cosmic-ray protons is $t_{GZK} \cong 140 \text{ Mpc}/c \cong 1.5 \times 10^{16}$ s.

The energy density u_{uhec} of GZK cosmic rays observed near Earth, as measured with the AGASA air shower array and the High Resolution air fluorescence detector [27], is $\approx 10^{-21}$ ergs cm^{-3} . If these cosmic rays are powered by GRBs with luminosity L_{GRB} throughout the universe, then

$$u_{uhec} \cong \zeta \frac{L_{GRB} t_{GZK}}{V_{prod}} \quad (5)$$

where V_{prod} is the production volume of the universe. Here UHECRs are assumed to be produced locally with an efficiency ζ compared with the mean γ -ray power of GRBs.

The mean γ -ray fluence of BATSE GRBs is $F_\gamma \approx 3 \times 10^{-6}$ ergs cm^{-2} and their rate over the full sky is $\dot{N}_{GRB} \approx 2/\text{day}$. If most GRBs are at redshift $\langle z \rangle \sim 1$, as implied by redshift measurements of GRBs detected with Beppo-SAX, which had similar triggering criteria as BATSE, then their mean distance is $\langle d \rangle \approx 2 \times 10^{28}$ cm. Thus the average isotropic energy release of a typical GRB source is $\langle E_\gamma \rangle \approx 4\pi \langle d \rangle^2 F_\gamma / (1+z) \cong 8 \times 10^{51}$ ergs, implying a mean GRB power into the universe of $L_{GRB} \approx 2 \times 10^{47}$ ergs s^{-1} . (This estimate is independent of the beaming fraction, because a smaller beaming fraction implies a proportionately larger number of sources.) This implies that the energy density observed locally is $u_{uhec} \approx 10^{-22} \zeta$ ergs cm^{-3} .

Thus super-GZK particles could in principle be powered by GRBs if roughly equal energies are deposited in super-GZK particles with energies exceeding 10^{20} eV as is

radiated by GRBs. Other effects, for example, bolometric corrections to the total photon fluence, the lower production rate of GRBs at $z \ll 1$ than at $z \approx 1$, the enhancement due to GRB-type sources which do not trigger GRB detectors, complicate the estimate.

In the model of Waxman and Bahcall [28], sources deposit UHECRs with energies between $\approx 10^{19}$ eV and 10^{21} eV with a -2 injection number spectrum. In this way, the coincidence is preserved, but the model requires a separate origin for UHECRs with energies below the cosmic-ray ankle energy of $\lesssim 5 \times 10^{18}$ eV. In their model, the ankle is interpreted as the energy of the transition between the galactic and extragalactic cosmic rays.

By contrast, in the model of Ref. [21], cosmic rays with energies between the knee at $\approx 3 \times 10^{15}$ eV and the second knee at $E_2 \approx 5 \times 10^{17}$ eV are mostly due to a single or a few relatively recent Galactic GRB/supernova events that occurred some $t_0 \lesssim 10^6$ yrs ago at distances $r_0 \lesssim 1$ kpc from us. UHECRs from extragalactic GRBs dominate at $E \gtrsim E_2$. This model explains the entire CR spectrum from GeV up to ultra-high energies (UHE) with a single population of sources, namely SNe. The coincidence between GRB electromagnetic power and UHECR power is however lost, and a large baryon load, $f_{CR} \gtrsim 20 - 50$, is required in GRBs, as compared to $f_{CR} \approx 1$ in Ref. [28], due to the softer spectrum and greater injection-energy range. The transition from galactic to extragalactic component takes place at the second knee of the cosmic-ray spectrum, in accord with indications for a change from heavy-to-light composition near the second knee [29]

A “single-source” model was proposed earlier by Erlykin and Wolfendale [30], who suggested that the knee could be due to a single “normal” supernova event that occurred some $t \sim 10^4$ yr ago within $r \sim 100$ pc from us. This differs from the approach of Ref. [21], because the latter model can explain acceleration of particles up to ultra-high energies by the relativistic shocks formed by GRB outflows, which is very problematic in the case of SNRs formed in the collapse to neutron stars. Moreover, the much larger total energy of cosmic rays injected by a SN/GRB, which permits the source to have occurred at larger (~ 1 kpc) distances and from a significantly older GRB than for a single normal SN source, makes it then easier to explain the likelihood of such an event, as well as the low degree of anisotropy observed in HECRs.

The model of Ref. [21] provides a way to explain the origin and the sharpness of the knee at $E_1 \simeq 3$ PeV as a consequence of pitch-angle scattering of cosmic rays on plasma waves injected in the interstellar medium (ISM) through dissipation of bulk kinetic energy of SNRs on the pc-scale Sedov length. Furthermore, the origin of the second knee in the cosmic-ray spectrum at $E_2 \simeq 4 \times 10^{17}$ eV is explained as a consequence of diffusive propagation through scattering with turbulence injected on a scale of ~ 100 pc, corresponding to the thickness of the Galactic disk, which perhaps represents the largest natural scale for effective injection of plasma turbulence in the Galaxy. The transition from Galactic to extragalactic CRs occurs around and above the second knee.

The rapid decline of the CR flux from local GRBs above the second knee results in the contribution of the extragalactic component to the all-particle spectrum dominating

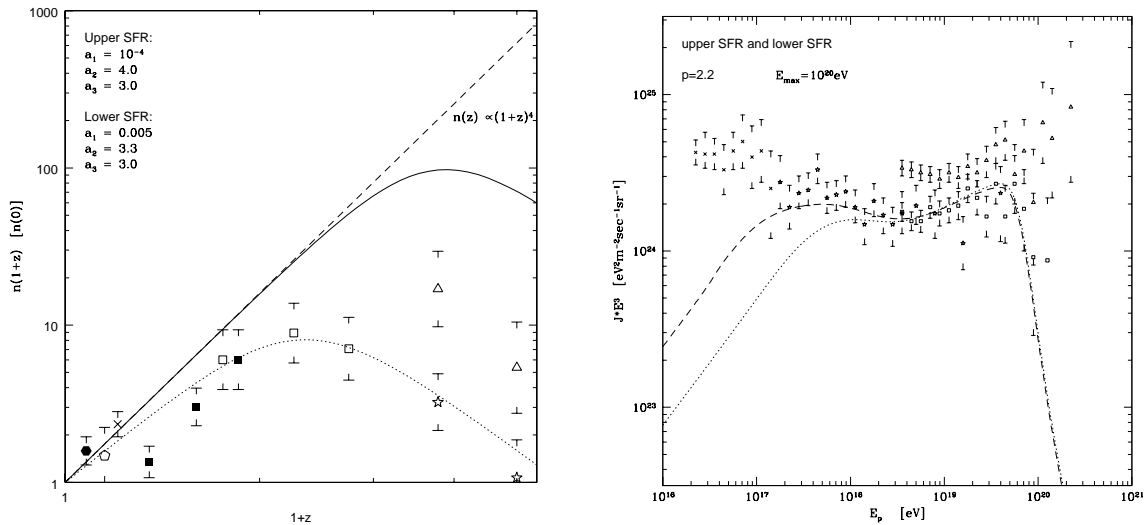


Figure 5. (a) (*left*) The history of evolution of the star formation rate (SFR) in the universe as a function of redshift $1+z$, normalized to the current SFR. The dotted curve shows the lower limit to the SFR evolution implied by measurements of the blue and UV energy density, and the solid curve shows the SFR corrected for dust extinction (see Ref. [21] for detailed discussion). The dashed line displays the relation $n(z) = n(0)(1+z)^4$ used by [9] for calculations of the fluxes of extragalactic CRs. (b) (*right*) Calculated fluxes of extragalactic CRs assuming that the injection of UHECRs in the universe was due to GRBs with a rate density proportional to the minimum (dotted curve) and maximum (solid curve) SFR functions shown in Fig. 5a. Note that the spectra are not normalized to each other at high energies. Instead, the normalization for both of them corresponds to the same value for the current ($z=0$) injection rate.

near and above the second knee. Calculations of the extragalactic component are shown in Fig. 5 for our model of CRs from GRBs, which includes photomeson interactions, $e^+ - e^-$ pair production, and adiabatic cooling of UHECRs [31, 7] during transport. We assume that the rate density of GRBs is proportional to the cosmological SFR of the universe. For the two rates shown in Fig. 5a that correspond to minimum and maximum SFRs, calculations in [21] result in the two spectra for the extragalactic component shown in Fig. 5b. An interesting result here is that in the framework of this model, the ankle in the spectrum of CRs observed at $E \simeq 3 \times 10^{18}$ eV is formed in the process of cooling of UHE protons on cosmological timescales.

Similar spectral behavior for the extragalactic CR component at $E \geq 10^{18}$ eV as shown in Fig. 5b, where the ankle is explained as a consequence of photopair losses of UHECRs formed at high redshift, was proposed also by Berezhinsky and collaborators [9]. They consider a model where UHECRs are accelerated by active galactic nuclei and assume cosmological evolution of the injection rate of UHECRs $\propto (1+z)^4$ (see Fig. 5a). It remains to be studied if these two principal options (GRBs and AGNs) for the sources of UHECRs in the universe can be distinguished from each other observationally as a result of differences in their evolutionary histories.

The spectra of UHECRs resulting from injection of UHECR protons in the universe

on cosmological timescales show a sharp (“GZK”) cutoff above the GZK energy $E \simeq 6 \times 10^{19}$ eV. The UHECR spectrum in Fig. 5b agrees with the HiRes data, but is in disagreement with the AGASA results at $E \gtrsim 10^{20}$ eV. If Auger observations show any significant excess over the exponential GZK cutoff at these energies, this would imply that there are other recent ($\lesssim 10^8$ yr) local source/sources of extragalactic origin in our vicinity at $\lesssim 10$ Mpc that produce this flux. One possibility is that the excess would be due to cosmic ray ions [32].

Extragalactic sources could be connected with starburst galaxies in the local group, such as M82 and NGC 253, both at distances $r \sim 3.5$ Mpc. Taking into account that the supernova rate in these galaxies is about 0.3 – 1 per year, and that the estimated GRB rate in our Galaxy is about (0.3 – 1)% of the supernova rate, the mean GRB rate in the starburst galaxies is estimated as one per $\sim 300 - 1000$ yrs. If the total energy of CRs accelerated by a typical GRB is indeed about 10^{52} ergs, as for our local Galactic GRB, the characteristic injection power of UHECRs from starburst galaxies averaged over the timescale of $\sim 10^8$ yr can be $\sim (1 - 3) \times 10^{42}$ ergs s $^{-1}$.

5. GRBs in the Local Universe

There are two important issues relevant to the question of the frequency and effects of GRBs in the Milky Way and the local universe. These are (1) the rate of GRBs as inferred from the GRB beaming factors; and (2) the dependence of GRBs on the SFR of the universe and the tendency of GRBs to be found in sites of different metallicity. These questions are crucial to determine at what rate GRBs occur in the Milky Way and whether they can be sources of cosmic rays above the knee of the cosmic ray spectrum. At the present time, it is not possible to answer either of these questions satisfactorily.

Regarding issue (1), achromatic beaming breaks in the afterglow light curves of GRBs can be used to infer the opening angle of the GRB jets. Direct observations [33] indicate that the mean measured opening angle is ≈ 0.1 radian, so that the opening angle of the GRB jets is $\approx 1/500^{th}$ of the full sky, leading to a rate of GRBs in the Milky Way Galaxy of 1 every 3,000 – 30,000 yrs [6]. A self-consistent calculation [34] for both the redshift and opening angle distribution suggests that the mean GRB opening angle is $\approx 1/75^{th}$ of the full sky, greatly reducing the rate in the Milky Way. The initial (prompt) opening angle of the GRB jet may, however, be smaller than the opening angles of the lower bulk-Lorentz factor outflows that produce, at later times, beaming breaks observed at optical frequencies, as in structured jet models (e.g., [35]). Hence the actual opening angles of the high Lorentz factor jets making the γ rays that trigger GRB detectors, and consequently define the rate of GRBs in the Milky Way, remains very uncertain.

The second important issue is whether GRBs follow the SFR of the universe, as shown in Fig. 5b, or follow a significantly different rate. If GRBs are the population of massive stars that collapse to black holes, then they may sample only a select portion of the high-mass stars that produce the blue/UV luminosity used to determine the SFR. If

the dependence of the GRB rate on the SFR changes with cosmic time, for example, due to the lower metallicities in the early universe, then the GRB rate in the recent epoch in the Milky Way may be much lower than inferred from the high-redshift GRBs [36, 37]. The tendency of GRBs to favor low-metallicity hosts is not certain because GRBs are preferentially found in OB associations [36], which may tend to have higher metallicity than the host galaxy; the host galaxy of GRB 980425 associated with SN 1998bw is a spiral galaxy with fairly high metallicity [37]; and high metallicity is found for GRB 060206 at redshift 4.048 from absorption line studies [38]. Moreover, the conclusions of [37] rest on only four GRBs with anomalously low beaming-corrected energies, which may simply indicate that underluminous GRBs have a tendency to be born in low metallicity environments.

Evidence for local GRBs can be established by identifying remnants of GRB in the Milky Way [39]. The identification of a ~ 1 Myr old GRB remnant (GRBR) that happened at a $\lesssim 1$ kpc from us, which explains [21] the origin of the knee(s) in the CR spectrum, is virtually impossible by now. However, there are other hopes to distinguish the radiation characteristics of the Galactic GRBRs from the radiation from the remnants of “ordinary” (nonrelativistic) supernovae in the Galaxy.

The HESS (High Energy Stereoscopic System) collaboration has recently discovered a population consisting of several γ -ray sources in the Galactic plane [40, 41], which are spatially extended—up to tens of arcmin—and TeV-bright, but are quiet in all other frequency bands and remain unidentified. The suppressed level of low-frequency synchrotron flux from TeV-bright sources is very unexpected for conventional SNRs. It is proposed in Ref. [42] through detailed calculations of particle diffusion and radiation processes and modeling of the spatial and spectral energy fluxes detected, that at least one of these sources, HESS J1303-631 [43], can be explained as a ~ 10 -20 kyr old GRBR at a distance ~ 10 -15 kpc from us. The hadronic origin of the detected TeV flux, implied by the non-detectable synchrotron flux, requires $\gtrsim 3 \times 10^{51}$ ergs energy in relativistic protons with $E > 5$ TeV. Furthermore, it is qualitatively argued [42] that the suppressed level of synchrotron flux could be the specific signature of the GRBRs. Unlike in the process of diffusive Fermi-type acceleration by nonrelativistic shocks for normal SNRs, the bulk kinetic energy of the relativistic shocks is converted to relativistic particles (mostly to protons rather than to electrons, because of the large difference in the rest masses) at the very early stages while the shock is relativistic. This can explain the large baryon load in the GRBs. Even at the early non-relativistic stage of evolution of the GRBR, the magnetic fields (~ 0.1 G) are still high and can quickly remove the relativistic leptons from the pool of accelerated particles. The most important observational feature predicted in [42] for the GRBRs, in contrast to SNRs, is the very hard spectrum of γ rays below 100 GeV energies. A weak detection, confirming the hard spectrum, or non-detection by GLAST of HESS J1303-631 would therefore signify detection of the signatures of proton acceleration by relativistic shocks of a GRB.

Confirmation of HESS J1303-631 and perhaps some other extended unidentified TeV source as GRBRs would confirm the high rate, of order 10^{-4} yr^{-1} , of local GRBs.

These questions are important for determining whether GRBs have had an impact upon the evolution of life at Earth [44, 6], as described in a related contribution to this focus issue [45].

6. Summary and Conclusions

The possibility that GRBs accelerate relativistic hadrons could solve the problem of the origin of the high-energy cosmic rays. There are several ways to establish whether GRBs accelerate cosmic rays, from: high-energy neutrino detection from GRBs; anomalous radiation signatures associated with hadronic acceleration and energy losses in GRB blast waves; radiations made by neutrons that escape from the blast wave; and evidence for cosmic-ray production from GRB remnants in our own and nearby galaxies.

In the case of neutrino and γ -ray production, at most only a few high-energy ν_μ can be detected with km-scale neutrino detectors even from bright GRBs at the fluence level $\Phi_{tot} \gtrsim 3 \times 10^{-4}$ erg cm $^{-2}$, and only when the baryon loading is high [13, 21]. This is because the detection of a single ν_μ requires a ν_μ fluence $\gtrsim 10^{-4}$ erg cm $^{-2}$ above 1 TeV. Since the energy release in high-energy neutrinos and electromagnetic secondaries is about equal, this energy will be reprocessed in the pair-photon cascade and emerge in the form of observable radiation at γ -ray energies, and this radiation cannot exceed the measured fluence in this regime. Detection of high-energy neutrinos and hadronic γ -ray emission components from GRBs will mean that GRBs have a large load in relativistic baryons, which is required for UHECR production.

The advent of the IceCube neutrino telescope at the South Pole and the launch of GLAST in late 2007 will provide the important instruments to establish whether GRBs accelerate ultra-relativistic hadrons. In the meantime, searches for GRB remnants at other wavelengths will indicate the importance of GRBs in the local universes. With these developments, the longstanding puzzle of the origin of the cosmic rays—now nearly 100 years since their discovery—should finally be answered.

We thank A. Reimer for permission to reproduce Fig. 1 from Ref. [10], and for useful comments on the manuscript. The work of C. D. D. is supported by the Office of Naval Research. We also acknowledge support of GLAST Science Investigation DPR-S-1563-Y.

References

- [1] Drury L O'C 1983 *Rep. Prog. Phys.* **46** 973
Ginzburg V L and Ptuskin V S 1985 *Astrophys. Sp. Phys. Rev.* **4** 161
- [2] Sommers P 2001 *27th International Cosmic Ray Conference* (Copernicus Gesellschaft, Hamburg, Germany) Invited, Rapporteur, and Highlight Papers, 170
Hörandel J R 2003 *Astropart. Phys.* **19** 193
- [3] Nagano M and Watson A A 2000 *Rev. Mod. Phys.* **72** 689
Waxman E 2004 *New Journal of Physics* **6** 140

- [4] Lagage P O and Cesarsky C J 1983 *Astron. Astrophys.* **125** 249
Baring M G, Ellison D C, Reynolds S P, Grenier I A, and Goret P 1999 *Astrophys. J.* **513** 311
- [5] Vietri M 1995 *Astrophys. J.* **453** 883
Waxman E 1995 *Phys. Rev. Letters* **75** 386
Waxman E 2004 *Astrophys. J.* **606** 988.
- [6] Dermer C D 2002 *Astrophys. J.* **574** 65
Dermer C D and Holmes J M 2005 *Astrophys. J. Lett.* **628** L21
- [7] Berezhinsky V S, Bulanov S V, Dogiel V A, Ginzburg V L, and Ptuskin V S 1990 *Astrophysics of Cosmic Rays* (Amsterdam: North Holland)
- [8] Atoyan A M and Dermer C D 2003 *Astrophys. J.* **586** 79
- [9] Berezhinsky V, Gazizov A, and Grigorieva S 2004, *Nuclear Phys. B* **136** 147
Berezhinsky V S, Gazizov A Z, and Grigorieva S I, 2005 *Phys. Lett. B* **612** 147
- [10] Mücke A, Rachen J P, Engel R, Protheroe R J, and Stanev T 1999 *Publ. Astron. Soc. Aust.* **16** 160
- [11] Baldini A, Flamini V, Moorhead W G, and Morrison D R O 1988 *Landolt-Börnstein New Ser. I/12b* ed. H Schopper (Berlin: Springer)
- [12] Hagiwara K *et al* 2002 *Phys. Rev. D* **66** 010001
- [13] Dermer C D and Atoyan A 2003 *Phys. Rev. Lett.* **91** 071102
- [14] Lock W O and Measday D F 1970 *Intermediate Energy Nuclear Physics* (Methuen: London) 1970
- [15] Mészáros P 2002 *Ann. Rev. Astron. Astrophys.* **40** 137
- [16] Waxman E and Bahcall J 1997 *Phys. Rev. Lett.* **78** 2292
Vietri M 1997 *Astrophys. J.* **478** L9
Böttcher M and Dermer C D 1998 *Astrophys. J. Lett.* **499** L131
- [17] Gallant Y A, Achterberg A, and Kirk J G 1999 *Astron. Astrophys. Supp.* **138** 549
- [18] Gaisser T K, Halzen F, and Stanev T 1995 *Phys. Repts.* **258(3)** 173
- [19] Atoyan A M and Dermer C D 2001 *Phys. Rev. Lett.* **87** 221102
- [20] Mücke, A., Engel, R., Protheroe, R. J., Rachen, J. P., & Stanev, T. 1999, *26th ICRC*, Salt Lake City, Utah, HE 4.2.10
- [21] Wick S D, Dermer C D, and Atoyan A 2004 *Astropart. Phys.* **21** 125
- [22] Dermer C D and Atoyan A 2004 *Astron. Astrophys.* **418** L5
- [23] González M, Dingus B, Kaneko Y, Preece R, Dermer C D, and Briggs M 2003 *Nature* **424** 749
González M 2005, PhD Thesis U. Wisconsin-Madison
- [24] Guetta D *et al.* 2004 *Astropart. Phys.* **20** 429
- [25] Greisen K 1966, *Phys. Rev. Lett.* **16** 748
Zatsepin G T and Kuzmin V A 1966 *JETP Lett.* **4** 78
- [26] Stanev T, Engel R, Mücke A, Protheroe, R J, Rachen J P 2000 *Phys. Rev. D* **62** 93005
- [27] T. Abu-Zayyad *et al.* 2004 *Phys. Rev. Lett.* **92** (2004) 151101
Takeda M, *et al* 1998 *Phys. Rev. Lett.* **81** 1163
- [28] Waxman E and Bahcall J N 1999 *Phys. Rev. D* **59** 023002
- [29] Bird D J *et al.* 1993 *Phys. Rev. Lett.* **71** 3401
- [30] Erlykin A D and Wolfendale A W 1997 *J. Phys. G: Nucl. Part. Phys.* **23** 979
- [31] Berezhinskii V S and Grigor'eva S I 1988 *Astron. Astrophys.* **199** 1
- [32] Allard D, Parizot E, Khan E, Goriely S, Olinto A V 2005 *Astron. Astrophys.*, submitted (*Preprint astro-ph/0505566*)
- [33] Frail D A *et al.* 2001 *Astrophys. J. Lett.* **562** L55
- [34] Guetta D, Piran T, and Waxman E 2005, *Astrophys. J.* **619** 412
- [35] Granot J and Kumar P 2006 *Monthly Not. Roy. Astron. Soc.* **366** L13
- [36] Fruchter A S *et al.* *Nature*, submitted (*Preprint astro-ph/0603537*)
- [37] Stanek K Z *et al.* *Astrophys. J.*, submitted (*Preprint astro-ph/0604113*)
- [38] Fynbo J P U *et al.* *Astron. Astrophys.*, submitted (*Preprint astro-ph/0602444*)
- [39] Loeb A and Perna R 1998 *Astrophys. J. Lett.* **503** L35

- [40] Aharonian F A *et al.* 2005 *Science* **307** 1839
- [41] Aharonian F A *et al.* 2006 *Astrophys. J.* **636** 777
- [42] Atoyan A, Buckley J, and Krawczynski H 2006 *Astrophys. J.*, **642**, 153
- [43] Aharonian F A *et al.* 2005 *Astron. Astrophys.* **439** 1013
- [44] Melott A L *et al.* 2004 *Internat. J. Astrobiology* **3** 55
- [45] Thomas B C and Melott A L 2006 *New Journal of Physics*